CLINICAL REPORT

Molecular Genetics & Genomic Medicine
Open Access WILEY

Long-read Oxford nanopore sequencing reveals a *de novo* case of complex chromosomal rearrangement involving chromosomes 2, 7, and 13

Lingling Xing[1,2] | Ying Shen[1,2] | Xiang Wei[1,2] | Yuan Luo[1,2] | Yan Yang[1,2] | Haipeng Liu[1,2] | Hongqian Liu[1,2]

[1]Department of Obstetrics and Gynaecology, West China Second University Hospital, Sichuan University, Chengdu, China

[2]Key Laboratory of Birth Defects and Related Diseases of Women and Children, Ministry of Education, Sichuan University, Chengdu, China

Correspondence
Hongqian Liu, Department of Obstetrics and Gynaecology, West China Second University Hospital, Sichuan University, Chengdu, China.
Email: hongqian.liu@163.com

Abstract

Background: Complex chromosomal rearrangements (CCRs) are associated with high reproductive risk, infertility, abnormalities in offspring, and recurrent miscarriage in women. It is essential to accurately characterize apparently balanced chromosome rearrangements in unaffected individuals.

Methods: A CCR young couple who suffered two spontaneous abortions and underwent labor induction due to fetal chromosomal abnormalities was studied using long-read sequencing(LRS), single-nucleotide polymorphism (SNP) array, G-banding karyotype analysis (550-band resolution), and Sanger sequencing.

Results: SNP analysis of the amniotic fluid cells during the third pregnancy revealed a 9.9-Mb duplication at 7q21.11q21.2 and a 24.8-Mb heterozygous deletion at 13q21.1q31.1. The unaffected female partner was a carrier of a three-way CCR [46,XX,? ins(7;13)(q21.1;q21.1q22)t(2;13)(p23;q22)]. Subsequent LRS analysis revealed the exact breakpoint locations on the derivative chromosomes and the specific method of chromosome rearrangement, indicating that the CCR carrier was a more complex structural rearrangement comprising five breakpoints. Furthermore, LRS detected an inserted fragment of chromosome 13 in chromosome 7.

Conclusions: LRS is effective for analyzing the complex structural variations of the human genome and may be used to clarify the specific CCRs for effective genetic counseling and appropriate intervention.

KEYWORDS
complex chromosomal rearrangements (CCRs), karyotype analysis of chromosome G-banding karyotype analysis (550 bands), long-read sequencing Oxford nanopore technology, third-generation sequencing (TGS)

1 | BACKGROUND

The main mechanisms of chromosome rearrangement include non-allelic homologous recombination (NAHR), non-homologous end joining (NHEJ), and fork stalling and template switching (FoSTeS). Simple balanced chromosomal rearrangement (BCR) refers to the rearrangement of two breakpoints, whereas complex chromosomal rearrangement (CCR) involves chromosomal abnormalities with three or more breakpoints, leading to the exchange of chromosomal fragments (Poot & Haaf, 2015). CCRs are relatively rare in the population, with approximately 380 reported cases (Aristidou et al., 2018; Liao et al., 2017), none of which include all of the three chromosomes presented in this case. CCRs often result in mental retardation, developmental delay, and multiple congenital abnormalities (MCA) in the affected offspring. When a CCR is detected in a phenotypically normal subject, the rearrangement is generally assumed to be balanced. Although most carriers of balanced CCRs have normal phenotypes, the risk of recurrent miscarriage, infertility, and having offspring with developmental defects is high (Kim et al., 2011; Pellestor et al., 2011). Depending on the degree of complexity, CCRs can be classified into three categories: (1) three-way rearrangements caused by three chromosomal breaks, resulting in a three-way exchange; (2) special translocation where each chromosome has more than one breakpoint, often combined with structural aberrations (e.g., translocation, inversion, insertion); and (3) double two-way translocations (i.e., coexistence of two or three simple reciprocities and Robertsonian translocations in the same carrier) (Pellestor et al., 2011). In terms of transmission, CCRs can be divided into familial and de novo cases.

Rearrangements related to the special mis-segregation pattern in meiosis contain more breaking points, and thus, pose a higher risk during reproduction. Gorski et al. first studied the pregnancy outcome of CCR carriers and discovered that the risk of miscarriage and pregnancy abnormality for couples with CCRs is estimated to be 48.3 and 53.7%, respectively (Gorski et al., 1988). However, this is a general rule; since most CCRs are unique in each family, it is strongly recommended that each CCR should be separately studied (Aristidou et al., 2018). Hence, to avoid birth defects, it is necessary to accurately characterize the karyotypes of CCR carriers with normal phenotypes to determine the reproductive risks and to choose the appropriate methods for a healthy pregnancy (e.g., spontaneous pregnancy combined with prenatal diagnosis, preimplantation genetic testing, use of donor sperm or egg) (Tan et al., 2020).

Accurate cytogenetic diagnosis depends on the resolution of the detection technology used. Previously, the identification of BCRs and confirmation of breakpoint regions were mainly based on the high-quality G-banding of metaphase chromosomes. However, due to the limited resolution of traditional cytogenetic techniques, only large structural rearrangements (>5 Mb) can be identified. Therefore, even with the use of high-resolution banding technology, the rearrangement of submicroscopic structures may still be undetectable. In clinical practice, conventional chromosome analysis via G-banding has been replaced by higher-resolution molecular techniques, including fluorescence in situ hybridization (FISH), chromosome microarray analysis (CMA), and whole-exome sequencing, to detect disease-causing mutations (e.g., copy number variations [CNVs], single-nucleotide variations). However, these techniques cannot recognize balanced translocations, inversions, and CCRs. Interestingly, recent studies have shown that similar to G-banding, whole-genome sequencing can detect extremely complex BCRs and locate molecular-level genomic structural variations (SVs) (Dong et al., 2019). Among these, third-generation sequencing (TGS) or long-read sequencing (LRS) has already been used for analyzing genomic rearrangements to identify the pathogenic variants (Merker et al., 2018; Sone et al., 2019). In recent years, with the development of high-throughput sequencing technology, TGS has gradually become an important method for genomic research. Among the current TGS technologies available, the single-molecule real-time (SMRT) sequencing technologies represented by Oxford Nanopore Technologies (ONT) and Pacific Biosciences (PacBio) can effectively solve several challenges in second-generation sequencing, such as covering highly repetitive genomes and complex regions and overcoming the preference bias caused by PCR amplification. Different from the PacBio sequencing principle, ONT sequencing is a new-generation SMRT electrical signal sequencing technology based on nanopores (Magi et al., 2018).

The ONT company has launched three main sequencing platforms—MinION, GridION, and PromethION. The PromethION sequencer platform (ONT, Oxford, UK) has high-throughput capability without GC preference, generates long reads, recognizes apparent modifications, effectively detects SVs, and provides other genomic information (De Coster et al., 2019). Recent studies have also demonstrated that nanopore long reads are superior to short reads in terms of detecting de novo chromothripsis rearrangements (Cretu Stancu et al., 2017). In addition, LRS of >10 kb-long reads is useful for characterizing CCRs since long reads may contain all or most of the complex rearrangements in the genome, effectively presenting the possible genetic variation involved. Furthermore, LRS can be used to determine the parental origin of new chromosomal breakpoints and solve the complex rearranged structures. Previous studies identified the reciprocal translocation breakpoints in the blood of BCRs by LRS Oxford Nanopore Technology (Hu et al., 2019; Pei et al., 2021).

However, CCRs were rarely analyzed by LRS. In our study, the PromethION sequencer with the largest throughput was used to analyze the structural characteristics of the detected CCRs with the aim of exploring the clinical utility of this technology for CCRs.

1.1 | Case presentation

A couple (II-1 and II-2 in Figure 1a), the male aged 28 years and the female aged 25 years, visited our hospital for genetic counseling and fertility guidance due to the increased thickness of the fetal nuchal translucency (NT). The ultrasound showed an NT of 0.63 cm when the female was pregnant for 20 + 2 weeks on September 10, 2020. Prior to this, two spontaneous abortions had occurred. In the third pregnancy, amniocentesis and CMA of amniotic fluid cells (AFCs) were performed. The pregnancy was terminated after the prenatal diagnosis showed an abnormal result. After genetic counseling, the couple underwent high-resolution G-banding karyotype analysis (550-band resolution), and the results showed that the unaffected female partner (II-2) was a carrier of a three-way CCR [46,

XX,? ins(7; 13)(q21.1;q21.1q22)t(2;13)(p23;q22)], whereas the male partner (II-1) has a normal karyotype (Figure 1b). To determine the source of the mutation, high-resolution G-banding was also conducted for the parents of the CCR carrier, but the results were normal. To accurately characterize the specific rearrangement in the CCR carrier, ONT sequencing was performed using the DNA from the peripheral blood lymphocytes of the female partner (II-2). We confirmed the potential breakpoint junctions via PCR amplification and subsequent Sanger sequencing to validate the results of ONT sequencing analysis. The study was approved by the Institutional Ethics Committee of Sichuan University, and all participants signed written informed consent prior to testing.

2 | MATERIALS AND METHODS

2.1 | Editorial policies and ethical considerations

This study was reviewed and approved by the Institutional Ethics Committee of Sichuan University. The patients/
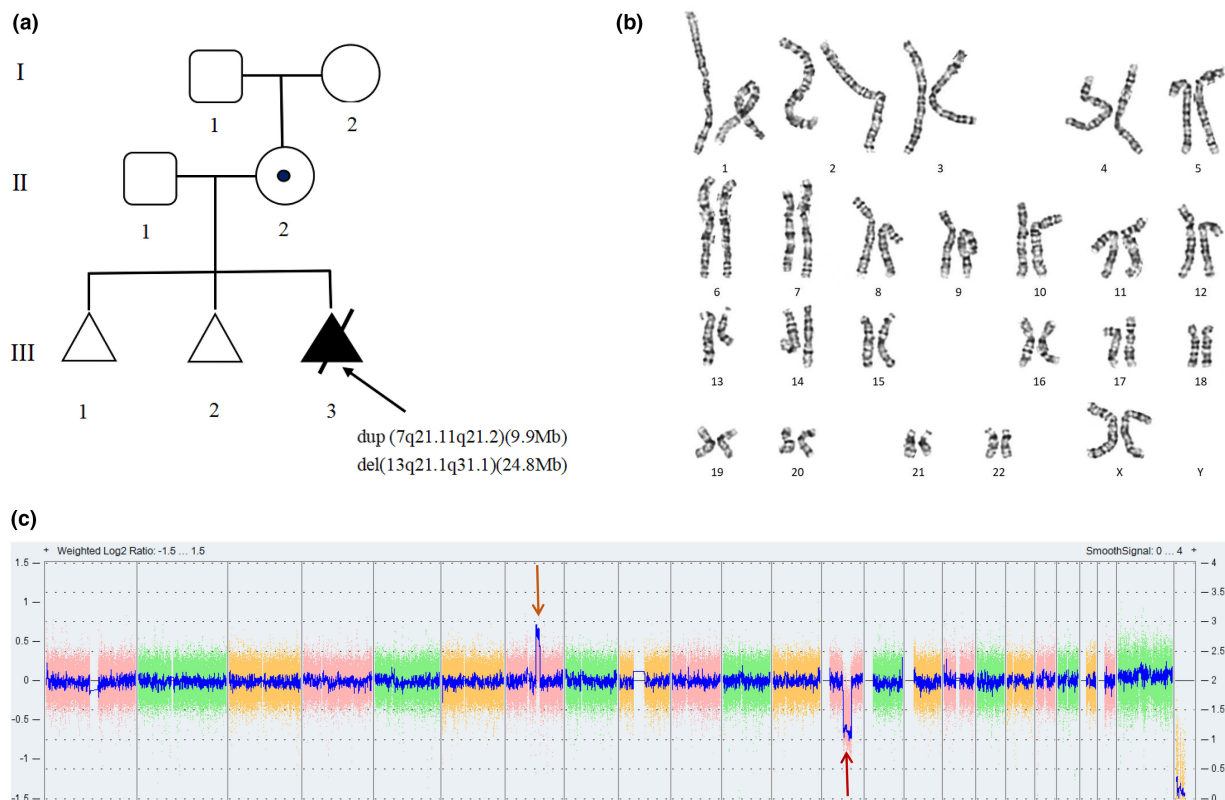

FIGURE 1 Molecular cytogenetic analysis of Family1. (a) Family pedigree of the proband (III-3, indicated by an arrow). Triangle, induced labor; circle with a black dot, female carrier; circles, females; squares, males. (b) Karyotype of the female carrier showing a complex translocation between chromosomes 2, 7, and 13, as detected by G-banding (550-band resolution). (c) Result of the CytoScan750K Array showing the signals of the duplication in chromosome 7 (orange arrow) and the deletion in chromosome 13 (red arrow).

participants provided their written informed consent to participate in this study.

2.2 | SNP array

SNP analysis was performed on individual III-3 using Cytoscan 750 K Array Chip (Affymetrix, Santa Clara, CA, USA). The data were analyzed with Chromosome Analysis Suite (ChAS) software (Affymetrix). Genomic DNA from AFCs was extracted using UPure Tissue DNA Kit (M2012-A96; Biobase, Sichuan, China) and KingFisher™ Flex System (Thermo Fisher Scientific, Waltham, MA, USA).

2.3 | G-banding karyotype analysis

The high-resolution G-banding karyotyping analysis of 550-band chromosomes was performed using the peripheral blood lymphocytes of individuals I-1, I-2, II-1, and II-2. The cell synchronization reagent was Chromed SK-A (Sinochrome/Cytogenetics, Shanghai, China). Metaphase cells were harvested using a Chromprep II automated cell harvester (Sinochrome/Cytogenetics, Shanghai, China). Data analysis was performed using the Metasystems Ikaros (ZEISS) chromosome automatic scanning analysis system.

2.4 | Long-read Oxford nanopore sequencing

In this study, the nanopore sequencing platform used for individual II-2 utilized the PromethION sequencer (ONT, Oxford, UK).

Genomic DNA was isolated from the peripheral blood lymphocytes. DNA purity was detected using Nanodrop (OD260/280 = 1.87, OD260/230 = 2.28); the degree of DNA degradation and RNA contamination were analyzed by pulsed-field gel electrophoresis and agarose gel electrophoresis; the DNA concentration was accurately quantified by Qubit (Qubit Concentration = 351 ng/ul). The DNA quality test results showed that the sample quality met the requirements for library construction and sequencing, and the total amount met the library construction requirements for one or more times. After the quality of the sample was evaluated, Megauptor® (Diagenode, Denville, NJ, USA) was used to break the DNA, with a break length of 30 kb. Long DNA fragments (>15 kb) were screened using BluePippin System (Sage Science, Beverly, MA, USA) and then purified. The purified DNA was subjected to end-repair and poly-A tail reaction experiments. After

purification, the DNA sample was mixed with the standard ONT sequencing adapters, motor proteins, and tether proteins. The prepared DNA library was sequenced using the PromethION platform. Nanopack, an official software package recommended by ONT (De Coster et al., 2018), was used to process the original offline data and to obtain high-quality sequencing data. The reads were mapped to the reference genome GRCh37/hg19 using Minimap2 (Li, 2018), and SAMtools (Li et al., 2009) was used to compare and sort the obtained BAM files. After bioinformatics analysis, we obtained a definite breakpoint area for further validation.

2.5 | Validation of the putative breakpoint regions

For primer design, the sequences (500 bp long) upstream and downstream of each putative breakpoint region were extracted based on the locations identified in the reference genome GRCh37/hg19. Primers were designed using Primer3 (http://primer3.ut.ee/), NCBI Primer-Blast (http://www.ncbi.nlm.nih.gov/tools/primer-blast/), and UCSC in silico PCR tool (https://genome.ucsc.edu/cgi-bin/hgPcr). PCR assays were performed using the specific primers for each sample, and the PCR products were sequenced via Sanger sequencing using ABI 3730 DNA Analyzer (Applied Biosystems, Thermo Fisher Scientific).

3 | RESULTS

The G-banding karyotype analysis (550-band resolution) showed that the male partner (II-1) had a normal karyotype, whereas the female partner (II-2) was a carrier of a three-way CCR, with the karyotype [46, XX,? ins(7;13)(q21.1;q21.1q22)t(2;13)(p23;q22)] (Figure 1b). Both parents (I-1 and I-2) of the female partner had normal karyotypes. Furthermore, SNP analysis using the AFCs revealed that the fetus (III-3) has an unbalanced chromosome rearrangement between chromosome 7, with a 9.9-Mb duplication at arr[GRCh37]7 q21.11q21.2(82514375_92480846)×3, and chromosome 13, with a 24.8-Mb deletion at arr[GRCh37]13q21 .1q31.1(56995788_81842703)×1 (Figure 1c).

To accurately determine the chromosomal rearrangement, the female partner was further subjected to ONT sequencing. The generation of ultra-long sequencing read length allowed the identification of 7698 deletions, 10,684 insertions, 80 repeats, and 60 inversions in the genome (Figure 2). Specifically, the intermediate segment 13q21.1–13q31.1 of the translocated chromosome 13 was inserted into the derivative chromosome 7. Notably, we
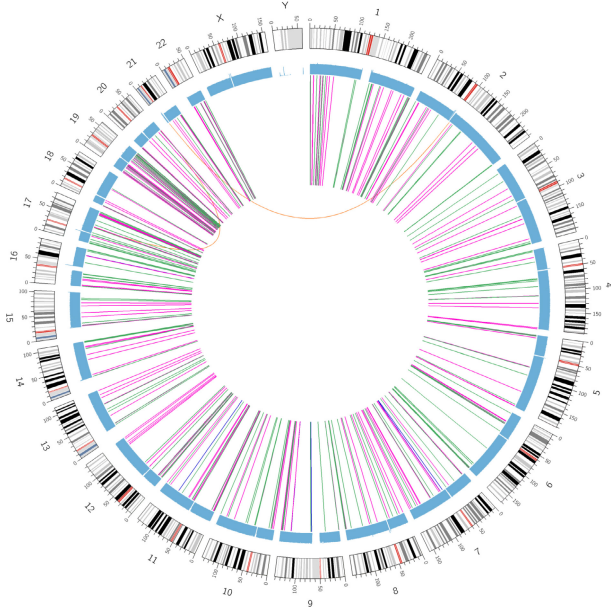
FIGURE 2 Circos plot of the identified structural variations (SVs). The first circle (outermost circle) represents the chromosome information, with 1–22, X, and Y representing the chromosomes and the numbers corresponding to the chromosome length in the karyotype. The second circle (blue circle) represents the sequencing coverage map, in which each 0.5-Mb is a unit calculating the average coverage. The third circle (innermost circle) shows the SVs detected in the genome. Due to the large number of SVs, only SVs located in the exonic, UTR, upstream, downstream, and splicing regions are displayed. Orange lines represent translocations, green lines represent deletions, blue lines represent inversions, and pink lines represent insertions/duplications. Chr, chromosome; svlen, length of structural variation; INS, insertion; DEL, deletion; DUP, duplication; INV, inversion; TRA, translocation.

confirmed that five breakpoints on chromosomes 2, 7, and 13 (2:18044504, 7:82511487, 7:92482297, 13:56958850, and 13:81861586) participated in the CCR and resulted in the disruption of the *PCLO* (MIM: 604918) gene. The breakpoints and mutual translocations on chromosomes 2, 7, and 13 were successfully characterized (Table 1, Figure 3). Finally, the derivative staining model of chromosomes 2, 7, and 13 was generated using the integrated karyotype analysis data and ONT sequencing results (Figure 4).

A gap-PCR assay was designed based on the results of deletion mapping to amplify the 300–700-bp fragment across the rearrangement breakpoints. Based on the genomic information, the PCR primers were designed to cover all breakpoint junctions (Table 2), and these five junctions were amplified via conventional PCR. As expected, amplicons showing the rearrangements were detected in the carrier when compared with the normal control. Three target fragments spanning the breakpoints were successfully amplified after the first PCR run (Figure 5a-1). After redesigning the primers, the

TABLE 1 Complete information of the breakpoints identified on chromosomes 2, 7, and 13

Chr	Start	End	Gene name	Func	Gene	CytoBand	CHR2	RE	AF	GT: DR: DV	SVTYPE
2	18,044,504	18,044,504		intergenic	NM_001105569; NM_001282428	2p24.2	7:82511487	17	0.809524	1/1:4:17	TRA
7	92,482,297	92,482,297	LOC101927497	ncRNA_intronic	NR_110086;NR_110087; NR_110088	7q21.2	13:81861586	25	0.714286	0/1:10:25	TRA
7	82,511,487	82,511,487	PCLO	intronic	NM_014510:NM_033026	7q21.11	13:56958850	10	0.555556	0/1:8:10	TRA

Notes: Func, region where the structural variation (SV) is located; GeneName, associated transcript ID; cytoBand, chromosomal location; RE, supported number of reads; AF, proportion of reads supporting the SV; GT:DR:DV: GT, Genotype (0 means Allele and REF are the same, 1, 2, 3, etc. means Allele and REF are different, 0/1 represents a heterozygous mutation, 1/1 represents a homozygous mutation [when the software detects a SV, 0.3 <AF≤0.8 is recorded as 0/1 and AF>0.8 is recorded as 1/1]); DR, sequencing depth of the reference base; DV, sequencing depth of the variant base; TRA, translocation.
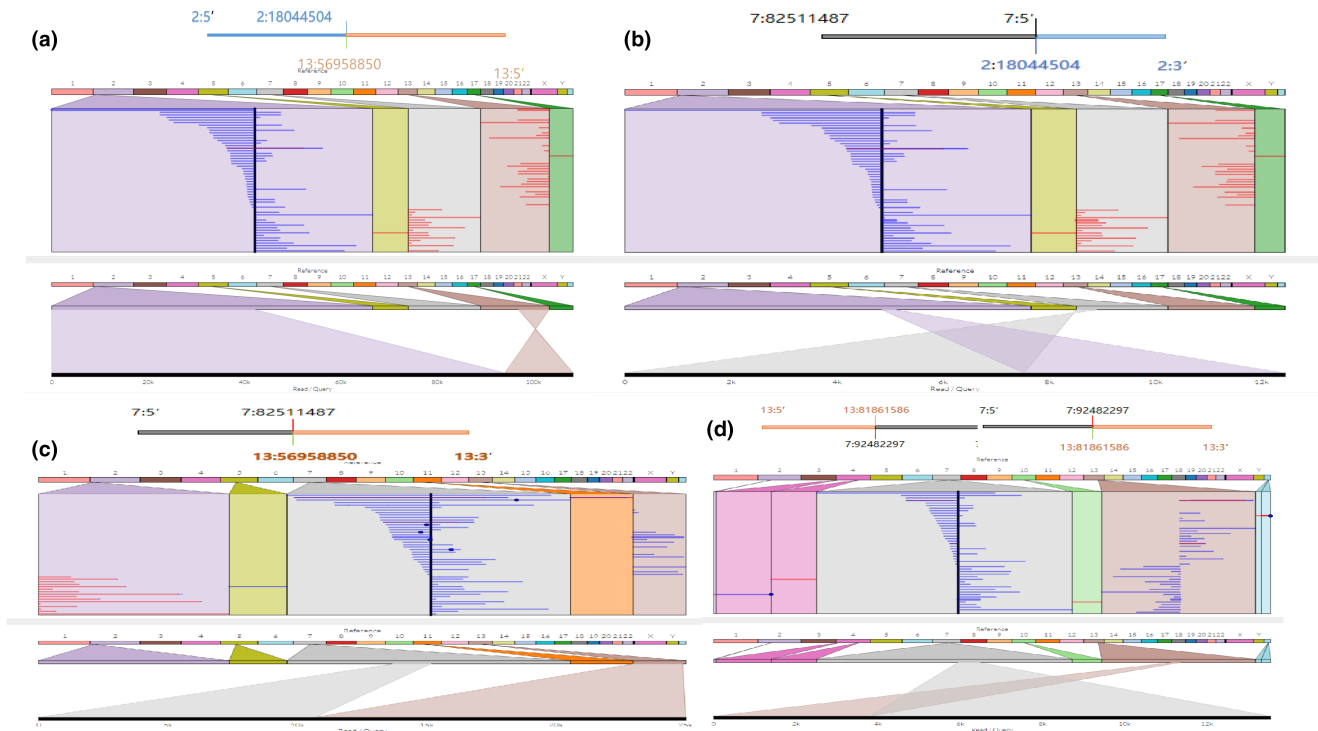
FIGURE 3 Visualization of the breakpoints in the target chromosomes. (a) The breakpoint upstream of chromosome 2 is connected to the breakpoint upstream of chromosome 13. (b) The chromosome 7 breakpoint is connected to the chromosome 2 breakpoint after being inverted upstream. (c) Translocation occurs to the breakpoints upstream of chromosome 7 and downstream of chromosome 13. (d) The structural variation at 7:92482297, representing the exchange of the two reads at the breakpoint.

remaining two target fragments were also successfully amplified (Figure 5a-2). Subsequent Sanger sequencing revealed the junction sequences at the nucleotide level (Figure 5b–f). Notably, micro-homologous sequences in the breakpoint region of the recombinant chromosome were also detected. Among these, the breakpoint region formed by chromosomes 2 and 13 contained a homologous sequence of approximately 130 bp. The final karyotype is specified as follows: 46,XX,der(2)(13qter → 13q31.1::7q21.2 → 7q21.11::2p24.2 → 2qter), der(7)(7pter → 7q21.11::13q21.1 → 13q31.1::7q21.2 → 7qter), der(13)(13pter → 13q21.1::2p24.2 → 2pter).

4 | DISCUSSION

Due to the associated high risk of recurrent spontaneous abortions and developing birth defects, it is necessary to detect CCRs in carriers with normal phenotypes since their offspring may inherit derivative chromosomes with CNVs. During meiosis, sister chromosomes involved in the insertion may form quadrivalents depending on the size of the inserted segment; reported cases of potential recombination involved relatively large insertion segments, with haploid autosomal length > 1.5%. Chromosome segregation following quadrivalent formation enables

potential recombination within the insertion segments to generate CCRs, resulting in copy number gains/losses (Dong et al., 2021). Furthermore, statistical analyses of the involvement and re-involvement of chromosomes in CCRs revealed that some chromosomes, such as chromosomes 2, 3, 4, 7, and 11, are more frequently implicated in CCRs than expected. Thus, the possibility that some chromosome loci may be "hotspots" for breakage and CCR formation has been postulated (Pellestor et al., 2011). In a study of four de novo cases and based on a literature review, Vermeulen et al. (2004) discovered that 30% of CCRs had breakpoints on chromosome 7, specifically on region 7q21.1, which contains genes involved in neuronal development (Vermeulen et al., 2004). Similarly, our study revealed that the CCR carrier had a breakpoint on 7q21.1.

In addition, the couple had a history of repeated spontaneous abortions, suggesting the need for cytogenetic testing. Previously, the identification of BCRs and confirmation of breakpoint regions were mainly based on the high-quality G-banding of metaphase chromosomes. However, traditional cytogenetic techniques can only identify large structural rearrangements (>5 Mb) due to their limited resolution. Therefore, even with the use of high-resolution banding technology, the rearrangement of submicroscopic structures may still be undetectable. Furthermore, fluorescence in situ hybridization (FISH)
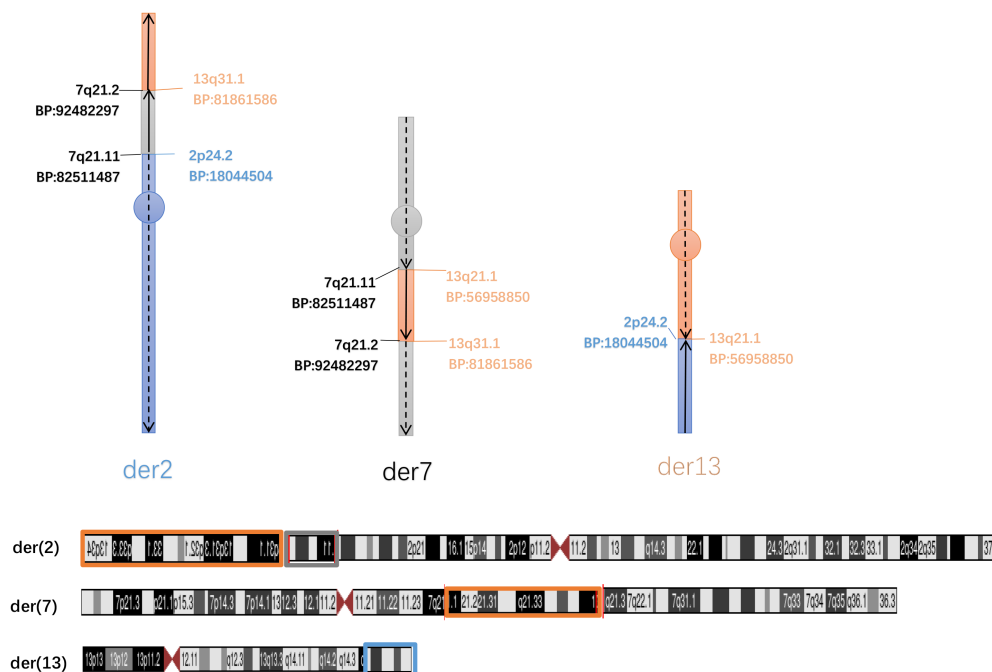
FIGURE 4 Derivative models of chromosomes 2, 7, and 13 from the complex chromosomal rearrangement (CCR) carrier in the family (II-2 in Figure 1a). Blue represents chromosome 2, gray represents chromosome 7, and orange represents chromosome 13. Dashed arrows indicate the direction of the chromosomal location in the original fragment of the derived chromosome (der), while solid arrows indicate the direction within the new fragment produced after breakpoint ligation. Two breakpoints may occur in the q or p arms of two non-homologous chromosomes (cis junctions) or genetic material may be exchanged between the q and p arms (trans junctions).

TABLE 2 Primers used for amplification of translocation breakpoints. F, forward primers; R, reverse primers; bp, base pairs

Primer		Primer sequence	Size of PCR products
juction1	F	TGGACTTGTGAATTACTGGAAGAA	749 bp
	R	CAGAGAAAAGAGGTATTTATTGGAGTT	
juction2	F	AGACCATTTTCATGGCATCTG	746 bp
	R	ACACAGTCCCTGCCTTGAGA	
juction3	F	CAAGAAATTTTTGAAGAATAGAACG	452 bp
	R	TGGAAATGCATATCTAAGGAAGG	
juction4	F	TGAAGTCAGCTTGTAAGTCCTTTTT	291 bp
	R	CATGAGTGAGATTAAATAAATGTTGG	
juction5	F	TCCCACTACCTGACATTTTGG	278 bp
	R	CCATCTTTTGCTCTGATCAATCT	

is the traditional approach for detecting translocations/inversions at the chromosome level. The resolution ratio of the FISH technique is approximately 100 kilobase to 1 megabase size (Cui et al., 2016), and it is more advantageous than karyotyping in BCR detection. However, FISH is unable to accomplish a precise translocation breakpoint analysis due to its requirements for specific fluorescent probes, complex procedures, and ambiguous fluorescence signals. In our study, karyotype analyses showed that the patient had CCRs and possessed

rearrangements involving chromosomes 2, 7, and 13. However, the CCR breakpoint-specific information cannot be clearly determined by karyotype analysis; therefore, we further used the LRS Oxford Nanopore Technology. Our results demonstrate the advantages of combining ONT sequencing with karyotyping: we not only detected large fragments of chromosome rearrangements and pinpointed the CCR breakpoints but also determined the changes in submicroscopic copy numbers, specifically the undetectable changes in the
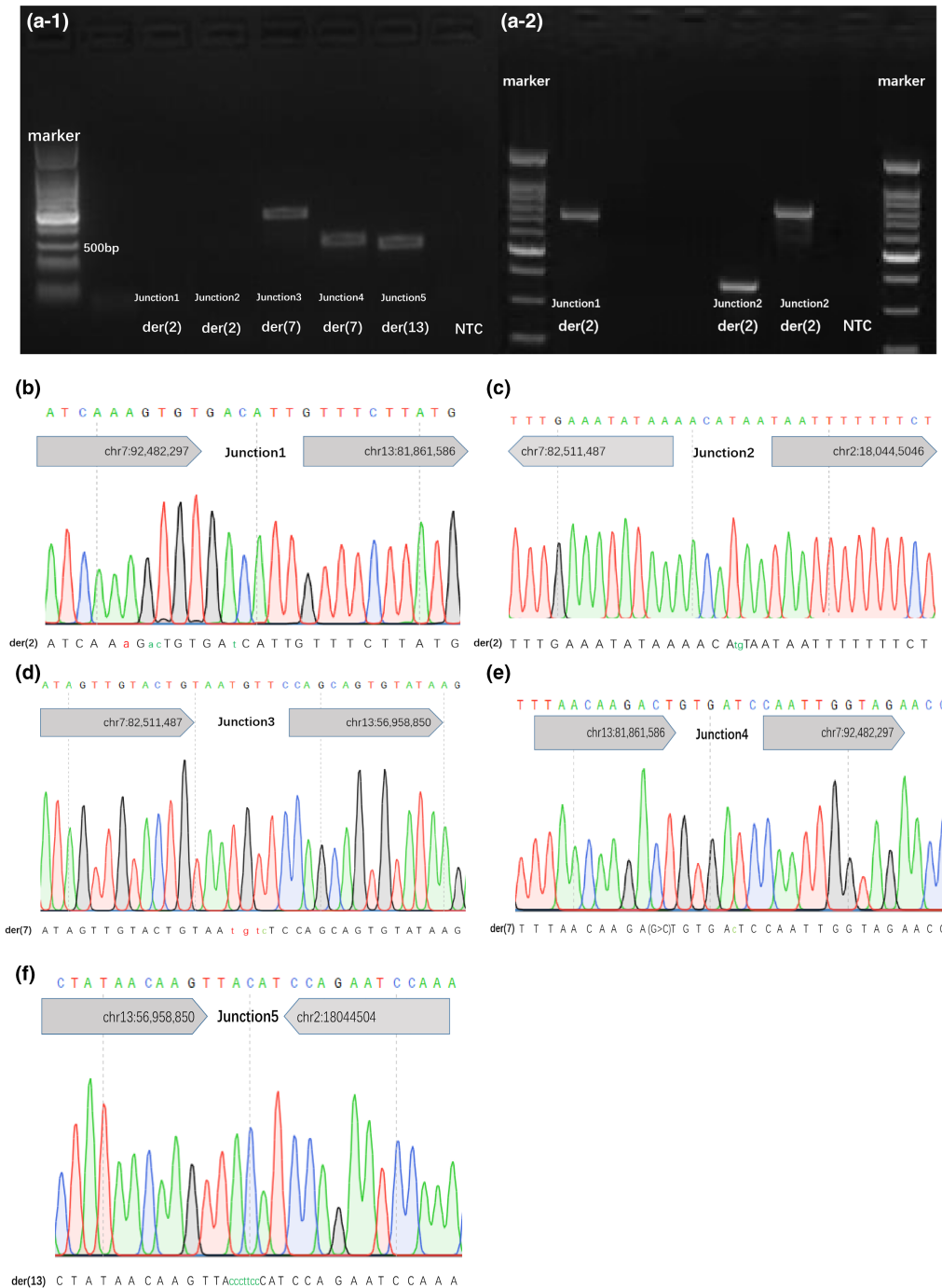
FIGURE 5 Validation of the putative breakpoint regions. (a) the five junction fragments were amplified, and the products were analyzed using 2% agarose gel electrophoresis. A normal sample was used as a negative control (NTC). (b–f) Chromatograms generated via sanger sequencing showing the breakpoints at the nucleotide level. Uppercase characters represent the original sequences, while lowercase/italicized characters represent the gained (red) or lost (green) bases.

genome structure. In our study, the CCR carrier karyotype (II-2) exhibited microhomology-mediated end joining patterns, in which a middle segment of chromosome 7 was inserted into chromosome 2 and a middle segment of chromosome 13 was inserted into chromosome 7. Previous studies have shown that insertions are rare three-break rearrangements with an incidence of

1/80,000 (Van Hemel & Eussen, 2000). Chromosomal insertion typically occurs during gametogenesis or meiosis, like other structural rearrangements. Simple insertions are primarily formed by three double-strand breaks and repaired via NHEJ (Bauters et al., 2008). The sequence patterns of breakpoint junctions after NHEJ may include blunt ends, short micro/small insertions,

and microhomologies. A subset of NHEJ is mediated by sequence microhomologies on both sides of the breakpoint, commonly termed as microhomology-mediated end joining (Ottaviani et al., 2014). The CCR with an inserted middle segment can produce new rearrangements, resulting in higher reproductive risk, increased unbalanced gamete production, and abnormal offspring.

Further research on submicroscopic chromosomal abnormalities may help explain the mechanisms involved in spontaneous abortions and birth defects and provide a basis for accurate genetic counseling. Accurate CCR models showing precise breakpoint sequences for use in subsequent preimplantation genetic testing for structural rearrangements (PGT-SR) may assist the embryo selection process. A more sophisticated version of PGT-SR can differentiate between euploid and balanced embryos by analyzing the sequences or genetic markers in and around breakpoint regions (Viotti, 2020). Nonetheless, the LRS Oxford Nanopore Technology has some drawbacks. First, due to the huge amount of data, the detection of rearrangements in large chromosome fragments using this method should be based on the results of karyotype analysis. Second, the method may not be able to detect Robertsonian translocation carriers because their breakpoints are in the highly repetitive centromeric regions of subtelocentric chromosomes. Third, it may bring new problems to the interpretation of results, such as determining the pathogenicity of small CNVs and detecting the changes in meiotic recombination patterns caused by SVs. Finally, its high economic costs may prevent it from becoming a first-line detection method.

In summary, in terms of chromosomal structural rearrangement, LRS is currently mainly used as a supplementary technology to accurately locate karyotype-prompted sites or to further mine suspicious variants in combination with other technologies, but it is not widely used in clinical practice. Our research shows that long-read Oxford Nanopore sequencing of peripheral blood lymphocytes from the CCR carrier revealed a large number of nucleotide variants that did not result in any clinical phenotype. Based on the high-resolution karyotype results, ONT sequencing can efficiently locate the breakpoints and produce ultra-long reads to accurately restore the recombinant chromosome model. We believe that in the future LRS may play a more important role in CCR analysis, as well as offer valuable insight for assisting reproduction and preimplantation genetic diagnosis. With the rapid development of LRS technology, the improvement of its sequencing accuracy, and the growing maturity of bioinformatics analysis, its large-scale clinical application may be just around the corner, which

will benefit more patients. Meanwhile, clinical genetic counseling will face greater challenges. In addition to objective factors (e.g., economic status, failure rate), the patient's prerogative must also be considered in choosing the appropriate assisted reproductive method (e.g., PGT-SR, egg donation).

CONFLICT OF INTEREST
This manuscript has not been published or presented elsewhere in part or in entirety and is not under consideration by another journal. All study participants provided informed consent, and the study design was approved by the appropriate ethics review board. There are no conflicts of interest to declare.

AUTHOR CONTRIBUTIONS
L.X. and H.L. designed the study. X.W. and Y.L., performed experiments. L.X, Y.S., Y.Y., H.L. analyzed the experimental results and data. L.X. wrote the main manuscript. H.L supervised the project and offered valuable suggestions for the revision of the manuscript. All authors participated in the discussion of the results and approved the final manuscript.

ETHICS STATEMENT
The studies involving human participants were reviewed and approved by the Institutional Ethics Committee of Sichuan University. The patients/participants provided their written informed consent to participate in this study.

DATA AVAILABILITY STATEMENT
The data analyzed in this study is subject to the following licenses/restrictions: the datasets for this article are not publicly available because of privacy concerns. Requests to access these datasets should be directed to HQL, hongqian.liu@163.com.

ORCID
Lingling Xing https://orcid.org/0000-0002-2235-6943
Ying Shen https://orcid.org/0000-0002-1484-0807

REFERENCES

Aristidou, C., Theodosiou, A., Ketoni, A., Bak, M., Mehrjouy, M. M., Tommerup, N., & Sismani, C. (2018). Cryptic breakpoint identified by whole-genome mate-pair sequencing in a rare paternally inherited complex chromosomal rearrangement. *Molecular Cytogenetics*, *11*, 34. https://doi.org/10.1186/s13039-018-0384-2

Bauters, M., Van Esch, H., Friez, M. J., Boespflug-Tanguy, O., Zenker, M., Vianna-Morgante, A. M., Rosenberg, C., Ignatius, J., Raynaud, M., Hollanders, K., Govaerts, K., Vandenreijt, K., Niel, F., Blanc, P., Stevenson, R. E., Fryns, J. P., Marynen, P., Schwartz, C. E., & Froyen, G. (2008). Nonrecurrent MECP2 duplications mediated by genomic architecture-driven DNA breaks and break-induced replication repair. *Genome Research*, *18*, 847–858. https://doi.org/10.1101/gr.075903.107

Cretu Stancu, M., van Roosmalen, M. J., Renkens, I., Nieboer, M. M., Middelkamp, S., de Ligt, J., Pregno, G., Giachino, D., Mandrile, G., Espejo Valle-Inclan, J., Korzelius, J., de Bruijn, E., Cuppen, E., Talkowski, M. E., Marschall, T., de Ridder, J., & Kloosterman, W. P. (2017). Mapping and phasing of structural variation in patient genomes using nanopore sequencing. *Nature Communications*, *8*, 1326. https://doi.org/10.1038/s41467-017-01343-4

Cui, C., Shu, W., & Li, P. (2016). Fluorescence in situ hybridization: Cell-based genetic diagnostic and research applications. *Frontiers in Cell and Developmental Biology*, *4*, 89. https://doi.org/10.3389/fcell.2016.00089

De Coster, W., De Rijk, P., De Roeck, A., De Pooter, T., D'Hert, S., Strazisar, M., Sleegers, K., & Van Broeckhoven, C. (2019). Structural variants identified by Oxford nanopore PromethION sequencing of the human genome. *Genome Research*, *29*, 1178–1187. https://doi.org/10.1101/gr.244939.118

De Coster, W., D'Hert, S., Schultz, D. T., Cruts, M., & Van Broeckhoven, C. (2018). NanoPack: Visualizing and processing long-read sequencing data. *Bioinformatics*, *34*, 2666–2669. https://doi.org/10.1093/bioinformatics/bty149

Dong, Z., Chau, M. H. K., Zhang, Y., Dai, P., Zhu, X., Leung, T. Y., Kong, X., Kwok, Y. K., Stankiewicz, P., Cheung, S. W., & Choy, K. W. (2021). Deciphering the complexity of simple chromosomal insertions by genome sequencing. *Human Genetics*, *140*, 361–380. https://doi.org/10.1007/s00439-020-02210-x

Dong, Z., Yan, J., Xu, F., Yuan, J., Jiang, H., Wang, H., Chen, H., Zhang, L., Ye, L., Xu, J., Shi, Y., Yang, Z., Cao, Y., Chen, L., Li, Q., Zhao, X., Li, J., Chen, A., Zhang, W., ... Chen, Z. J. (2019). Genome sequencing explores complexity of chromosomal abnormalities in recurrent miscarriage. *American Journal of Human Genetics*, *105*, 1102–1111. https://doi.org/10.1016/j.ajhg.2019.10.003

Gorski, J. L., Kistenmacher, M. L., Punnett, H. H., Zackai, E. H., & Emanuel, B. S. (1988). Reproductive risks for carriers of complex chromosome rearrangements: Analysis of 25 families. *American Journal of Medical Genetics*, *29*, 247–261. https://doi.org/10.1002/ajmg.1320290202

Hu, L., Liang, F., Cheng, D., Zhang, Z., Yu, G., Zha, J., Wang, Y., Xia, Q., Yuan, D., Tan, Y., Wang, D., Liang, Y., & Lin, G. (2019). Location of balanced chromosome-translocation breakpoints by long-read sequencing on the Oxford nanopore platform. *Frontiers in Genetics*, *10*, 1313. https://doi.org/10.3389/fgene.2019.01313

Kim, J. W., Chang, E. M., Song, S. H., Park, S. H., Yoon, T. K., & Shim, S. H. (2011). Complex chromosomal rearrangements in infertile males: Complexity of rearrangement affects spermatogenesis. *Fertility and Sterility*, *95*, 349–352.e1. https://doi.org/10.1016/j.fertnstert.2010.08.014

Li, H. (2018). Minimap2: Pairwise alignment for nucleotide sequences. *Bioinformatics*, *34*, 3094–3100. https://doi.org/10.1093/bioinformatics/bty191

Li, H., Handsaker, B., Wysoker, A., Fennell, T., Ruan, J., Homer, N., Marth, G., Abecasis, G., Durbin, R., & 1000 Genome Project Data Processing Subgroup. (2009). The sequence alignment/map format and SAMtools. *Bioinformatics*, *25*, 2078–2079. https://doi.org/10.1093/bioinformatics/btp352

Liao, Y. P., Wang, C. J., Liang, M., Hu, X. M., & Wu, Q. (2017). Analysis of genetic characteristics and reproductive risks of balanced complex chromosome rearrangement carriers in China. *Yi Chuan*, *39*, 396–412. https://doi.org/10.16288/j.yczz.16-322

Magi, A., Semeraro, R., Mingrino, A., Giusti, B., & D'Aurizio, R. (2018). Nanopore sequencing data analysis: State of the art, applications and challenges. *Briefings in Bioinformatics*, *19*, 1256–1272. https://doi.org/10.1093/bib/bbx062

Merker, J. D., Wenger, A. M., Sneddon, T., Grove, M., Zappala, Z., Fresard, L., Waggott, D., Utiramerur, S., Hou, Y., Smith, K. S., Montgomery, S. B., Wheeler, M., Buchan, J. G., Lambert, C. C., Eng, K. S., Hickey, L., Korlach, J., Ford, J., & Ashley, E. A. (2018). Long-read genome sequencing identifies causal structural variation in a mendelian disease. *Genetics in Medicine: Official Journal of the American College of Medical Genetics*, *20*, 159–163. https://doi.org/10.1038/gim.2017.86

Ottaviani, D., LeCain, M., & Sheer, D. (2014). The role of microhomology in genomic structural variation. *Trends in Genetics: TIG*, *30*, 85–94. https://doi.org/10.1016/j.tig.2014.01.001

Pei, Z., Deng, K., Lei, C., Du, D., Yu, G., Sun, X., Xu, C., & Zhang, S. (2021). Identifying balanced chromosomal translocations in human embryos by Oxford nanopore sequencing and breakpoints region analysis. *Frontiers in Genetics*, *12*, 810900. https://doi.org/10.3389/fgene.2021.810900

Pellestor, F., Anahory, T., Lefort, G., Puechberty, J., Liehr, T., Hédon, B., & Sarda, P. (2011). Complex chromosomal rearrangements: Origin and meiotic behavior. *Human Reproduction Update*, *17*, 476–494. https://doi.org/10.1093/humupd/dmr010

Poot, M., & Haaf, T. (2015). Mechanisms of origin, phenotypic effects and diagnostic implications of complex chromosome rearrangements. *Molecular Syndromology*, *6*, 110–134. https://doi.org/10.1159/000438812

Sone, J., Mitsuhashi, S., Fujita, A., Mizuguchi, T., Hamanaka, K., Mori, K., Koike, H., Hashiguchi, A., Takashima, H., Sugiyama, H., Kohno, Y., Takiyama, Y., Maeda, K., Doi, H., Koyano, S., Takeuchi, H., Kawamoto, M., Kohara, N., Ando, T., ... Sobue, G. (2019). Long-read sequencing identifies GGC repeat expansions in NOTCH2NLC associated with neuronal intranuclear inclusion disease. *Nature Genetics*, *51*, 1215–1221. https://doi.org/10.1038/s41588-019-0459-y

Tan, Y. Q., Tan, Y. Q., & Cheng, D. H. (2020). Whole-genome mate-pair sequencing of apparently balanced chromosome rearrangements reveals complex structural variations: Two case studies. *Molecular Cytogenetics*, *13*, 15. https://doi.org/10.1186/s13039-020-00487-1

Van Hemel, J. O., & Eussen, H. J. (2000). Interchromosomal insertions. Identification of five cases and a review. *Human Genetics*, *107*, 415–432. https://doi.org/10.1007/s004390000398

Vermeulen, S., Menten, B., Van Roy, N., Van Limbergen, H., De Paepe, A., Mortier, G., & Speleman, F. (2004). Molecular cytogenetic analysis of complex chromosomal rearrangements in patients with mental retardation and congenital malformations: Delineation of 7q21.11 breakpoints. *American Journal of Medical Genetics. Part A*, *124A*, 10–18. https://doi.org/10.1002/ajmg.a.20378

Viotti, M. (2020). Preimplantation genetic testing for chromosomal abnormalities: Aneuploidy, mosaicism, and structural rearrangements. *Genes (Basel)*, *11*(6), 602. https://doi.org/10.3390/genes11060602